International Journal of Heat and Mass Transfer 64 (2013) 1226–1238

Contents lists available at SciVerse ScienceDirect

International Journal of Heat and Mass Transfer

journal homepage: www.elsevier.com/locate/ijhmt

Universal approach to predicting saturated flow boiling heat transfer in mini/micro-channels – Part I. Dryout incipience quality

Sung-Min Kim, Issam Mudawar *

Boiling and Two-Phase Flow Laboratory (BTPFL) and Purdue University International Electronic Cooling Alliance (PUIECA), Mechanical Engineering Building, 585 Purdue Mall, West Lafayette, IN 47907-2088, USA

ARTICLE INFO

Article history:
Available online 30 April 2013

Keywords:
Dryout incipience
Two-phase flow
Flow boiling
Mini-channel
Micro-channel

ABSTRACT

This two-part study concerns the development of a generalized approach to predicting both Nucleate Boiling dominated and Convective Boiling dominated heat transfer in mini/micro-channel flows. Both heat transfer regimes exhibit substantial reduction in the heat transfer coefficient at the location of partial annular liquid film dryout, hence the need to ascertain the occurrence of this important transition point. This first part of the study concerns the development of a correlation for dryout incidence quality. This goal is accomplished by first amassing a consolidated database consisting of 997 dryout data points for mini/micro-channels from 26 sources. The database includes 13 different working fluids, hydraulic diameters from 0.51 to 6.0 mm, mass velocities from 29 to 2303 kg/m^2 s, liquid-only Reynolds numbers from 125 to 53,770, Boiling numbers from 0.31×10^{-4} to 44.3×10^{-4}, and reduced pressures from 0.005 to 0.78. The new dimensionless correlation is comprised of Weber, Capillary and Boiling numbers, reduced pressure, and density ratio. The correlation shows good predictions of the entire database, evidenced by an overall MAE of 12.5%, and 93.6% and 98.0% of the predictions falling within ±30% and ±50% of the data, respectively. The predictive accuracy of the new correlation is also fairly even for the 13 different working fluids, and over broad ranges of all relevant parameters.

© 2013 Elsevier Ltd. All rights reserved.

1. Introduction

Advances in many modern applications, such as computer data centers, avionics, lasers and X-ray medical systems, are becoming increasingly dependent on the ability to dissipate large amounts of heat from small surface areas. This explains the quest for high heat flux thermal management solutions using a variety of two-phase cooling schemes, including pool boiling [1,2], mini/micro-channel flow [3–5], jet [6–9] and spray [10–13]. Efforts also included means to enhance cooling performance by the use of enhanced surfaces [14–16], and hybrid cooling techniques that combine the benefits of two or more cooling schemes [17,18].

Among these cooling schemes, two-phase mini/micro-channel devices have been the target of intense study because of their ability to offer a number of unique attributes, such as compactness, relative ease of fabrication, high heat dissipation to volume ratio, and small coolant inventory. This is manifest in the unusually large number of articles that have been written on this topic, addressing both pressure drop and heat transfer characteristics of flow boiling in small channels. But rather than providing systematic predictive tools, the large number of articles has led to appreciable confusion about which tools thermal system designers must use. Clearly, there is now an urgent need to consolidate published findings in pursuit of 'universal' predictive tools that are applicable to different working fluids and broad ranges of operating conditions.

The development of this type of predictive tool is the primary motivation for a series of studies that have been initiated at the Purdue University Boiling and Two-Phase Flow Laboratory (PU-BTPFL), which involve systematic consolidation of world databases for mini/micro-channels, and development of universal predictive tools for pressure drop [19,20] and condensation heat transfer coefficient [21], following very closely a methodology that was adopted earlier to predict flow boiling critical heat flux (CHF) for water flow in tubes [22–24].

The present study concerns the development of similar universal predictive tools for heat transfer in mini/micro-channel flows that cover working fluids with drastically different thermophysical properties and broad ranges of mass velocity, pressure, and channel diameter. But, before discussing the development of these predictive tools, it is important to discuss differences in the manner dryout and CHF in mini/micro-channel flows are identified by previous authors since these phenomena constitute important boundaries to two-phase heat transfer performance.

CHF is highly dependent on inlet subcooling of the working fluid. For subcooled boiling, four different mechanisms have been proposed to trigger CHF: Boundary Layer Separation, Bubble

* Corresponding author. Tel.: +1 (765) 494 5705; fax: +1 (765) 494 0539.
E-mail address: mudawar@ecn.purdue.edu (I. Mudawar).
URL: https://engineering.purdue.edu/BTPFL (I. Mudawar).

0017-9310/$ - see front matter © 2013 Elsevier Ltd. All rights reserved.
http://dx.doi.org/10.1016/j.ijheatmasstransfer.2013.04.016

Nomenclature

A	flow area
Bd	Bond number
Bo	Boiling number, q''_H/Gh_{fg}
Ca	Capillary number
D	tube diameter
D_h	hydraulic diameter
e	surface roughness
Fr	Froude number
Fr^*	modified Froude number
G	mass velocity
g	gravitational acceleration
h_{fg}	latent heat of vaporization
h_{tp}	two-phase heat transfer coefficient
MAE	mean absolute error
N	number of data points
P	pressure
P_{crit}	critical pressure
P_F	wetted perimeter of channel
P_H	heated perimeter of channel
P_R	reduced pressure, $P_R = P/P_{crit}$
q''	heat flux
q''_H	heat flux based on heated perimeter of channel
Re	Reynolds number
Re_{fo}	liquid-only Reynolds number, $Re_{fo} = GD_h/\mu_f$
T	temperature
$T_{w,std}$	standard deviation of wall temperature
We	Weber number
x	thermodynamic equilibrium quality
x_{crit}	dryout completion (CHF) quality
x_{di}	dryout incipience quality
z	stream-wise coordinate

Greek symbols

θ	percentage predicted within ±30%; channel inclination angle
μ	dynamic viscosity
ξ	percentage predicted within ±50%
ρ	density
σ	surface tension

Subscripts

b	bottom of micro-channel
$base$	base area of micro-channel heat sink
$crit$	critical
exp	experimental (measured)
f	saturated liquid
fo	liquid only
g	saturated vapor
in	inlet
$pred$	predicted
sat	saturation
tp	two-phase
w	wall

Crowding, Sublayer Dryout, and Interfacial Lift-off. The Boundary Layer Separation Model is based on the assumption that CHF occurs when the rate of vapor effusion normal to the heated wall reaches a threshold that causes the liquid velocity gradient near the wall to become very small, resulting in separation of the liquid from the wall [25,26]. The Bubble Crowding Model is based on the assumption that CHF occurs when turbulent fluctuations in the core liquid flow become too weak to allow liquid to penetrate the thick bubbly wall layer and supply adequate liquid to the wall [27,28]. The Sublayer Dryout Model is based on the premise that CHF commences when the heat supplied at the wall exceeds the enthalpy of liquid replenishing a thin sublayer beneath long, coalescent vapor bubbles at the wall [29]. The Interfacial Lift-off Model is built upon the observation that the vapor coalesces into a fairly continuous vapor layer before CHF [30–33]. The wavy interface between the core liquid and vapor layer is able to make contact with the heated wall in the wave troughs to provide adequate cooling, and CHF occurs when the wave troughs are lifted away from the wall due to intense vapor effusion.

Dryout is more closely associated with saturated inlet conditions and development of a clearly identifiable annular flow regime. Fig. 1(a) and (b) shows schematics of two types of heat transfer regimes that are associated with saturated inlet conditions and terminated with dryout. The first, Fig. 1(a), is *Nucleate Boiling Dominant* heat transfer (e.g. [34–36]), where bubbly and slug flow regimes occupy a significant portion of the channel length, and the heat transfer coefficient decreases due to gradual suppression of nucleate boiling. In contrast, Fig. 1(b) depicts *Convective Boiling Dominant* heat transfer (e.g. [37–39]), where annular flow spans a significant fraction of the channel length. Here, gradual evaporation and thinning of the annular liquid film causes the heat transfer coefficient to increase along the channel length. With a sufficiently high wall heat flux or sufficiently long channel, the annular film becomes vanishingly thin for both heat transfer regimes. A lack of perfect symmetry in the film flow or uneven evaporation causes initial dry patches to form at the location of *Dryout Incipience* (i.e., onset of dryout, or partial dryout), where the heat transfer coefficient begins to decrease appreciably. Eventually, *Dryout Completion* occurs at a location farther downstream, where the film is fully evaporated.

Prior authors have adopted different guidelines to identifying dryout incipience and dryout completion conditions. According to Martín-Callizo [36] and Ali and Palm [40], dryout incipience could be identified from a shift in the slope of the measured boiling curve with increasing heat flux, where wall temperature starts to increase steeply following a small heat flux increment. This slope change occurs before the large temperature excursion attributed to dryout completion and commonly referred to as CHF. They attributed the slope change corresponding to dryout incipience to intermittent dry patches that begin to appear in the annular film. Unfortunately, the distinction between dryout incipience and dryout completion in published studies is quite elusive and often not clearly pointed out. Differences between heat fluxes corresponding to these two conditions are greatly influenced by working fluid, as shown in Fig. 2(a) and (b). Fig. 2(a) shows a boiling curve measured by Qu and Mudawar [41] for water flow boiling in rectangular micro-channels in which CHF corresponding to dryout completion was clearly measured by a sharp and unsteady wall temperature excursion. Both the dryout incipience and dryout completion heat fluxes are clearly identified and shown encompassing a narrow dryout region. On the other hand, Fig. 2(b) shows a boiling curve measured by Lee and Mudawar [42] for flow boiling of R134a in rectangular micro-channels. Here, dryout incipience and dryout completion encompass a broad heat flux range corresponding to the dryout region. The narrow dryout region depicted in Fig. 2(a) is typical of micro/mini-channel water data and is largely the result of the high latent heat and high CHF values for water, and corresponding fast wall temperature excursion at

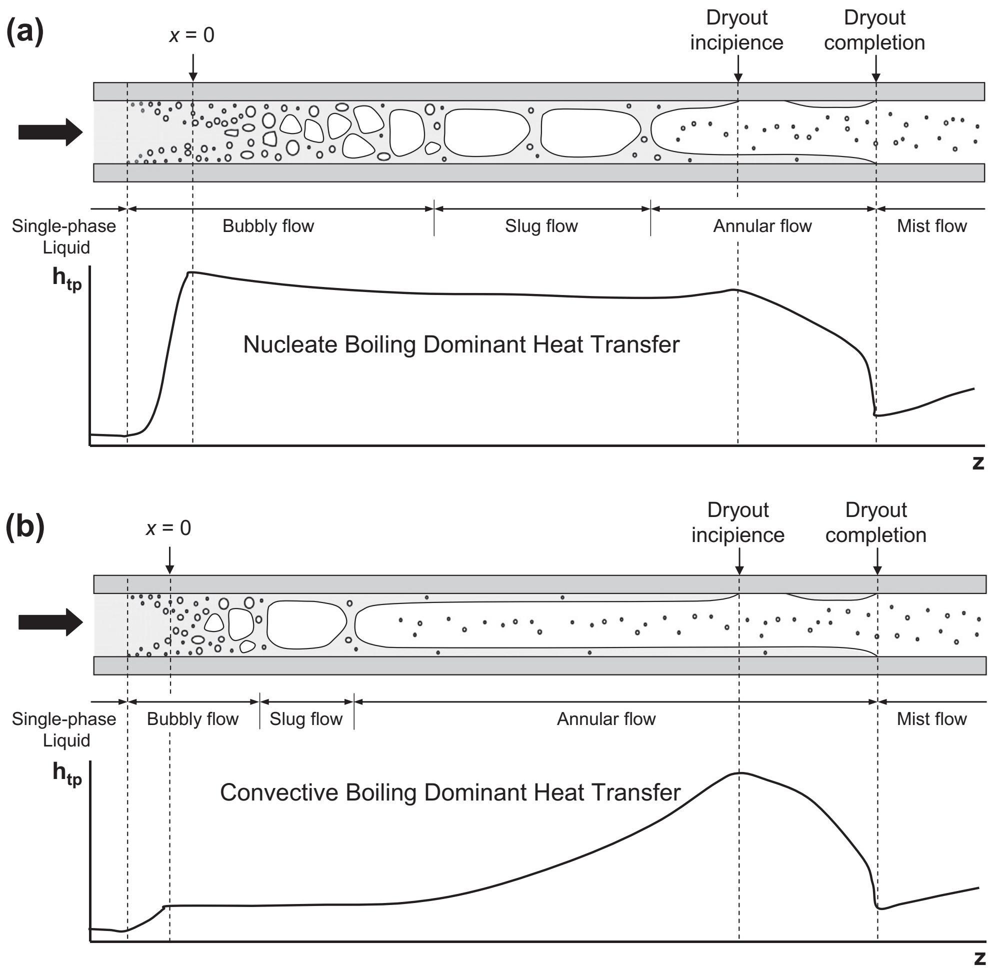

Fig. 1. Schematics of flow regimes, wall dryout and variation of heat transfer coefficient along uniformly heated channel for (a) nucleate boiling dominant heat transfer and (b) convective boiling dominant heat transfer.

CHF. On the other hand, the relatively broad dryout region depicted in Fig. 2(b) is representative of data for refrigerants and dielectric fluids, which possess relatively low latent heat and low CHF values, and exhibit slow temperature excursion at CHF.

This first part of a two-part study examines dryout phenomena for saturated flow boiling in mini/micro-channels. The primary objective of the second part of this study [43] is to develop a generalized pre-dryout saturated flow boiling heat transfer correlation for mini/micro-channels. Since many published studies include data downstream of dryout incipience (i.e., partial dryout as well as post-dryout data), it is crucial to exclude those data points from the original databases when developing a predictive method for the pre-dryout heat transfer coefficient.

The primary goal of the present study is to develop a generalized correlation for dryout incipience quality for flow boiling in mini/micro-channels that is applicable to working fluids with drastically different thermophysical properties and to broad ranges of operating conditions. This goal is achieved by, first, amassing published dryout incipience quality and dryout completion quality (CHF) data for flow boiling in mini/micro-channel flows from 26 sources [34–40,44–62]. The consolidated database is then compared to predictions of previous dryout incipience quality correlations [56,61,63–69]. Finally, a new generalized correlation is proposed that is shown to predict dryout incipience quality data with superior accuracy.

2. New consolidated mini/micro-channel database

A new consolidated database consisting of 997 data points for dryout incipience quality, x_{di}, and dryout completion quality (CHF), x_{crit}, in mini/micro-channels is amassed from 26 sources [34–40,44–62]. Table 1 provides key information on the individual databases comprising the consolidated database in chronological order. The database consists of 664 data points for water from six sources, and 333 data points for other fluids from 20 sources. The water data of Becker [44], Lezzi et al. [45], Baek and Chang [46], Roach et al. [47], Kim et al. [48], and Yu et al. [50] correspond to dryout completion quality at which CHF occurs. Notice that different criteria where adopted by individual authors to determine CHF and therefore the corresponding dryout completion quality, x_{crit}. For example, Lezzi et al. [45] identified CHF by a 5 °C increase in average wall temperature following a small heat flux increment and long waiting period. On the other hand, Baek and Chang [46] identified CHF as occurring when the wall temperature exceeded a fairly high limit of 250 °C. Therefore, the CHF criterion of Lezzi et al. is in fact more closed related to dryout incipience, while the CHF criterion of Baek and Chang is indicative of dryout completion, or true CHF. Since, as shown in Fig. 2(a), the dryout incipience and dryout completion conditions are quite close for water, the data for dryout completion quality, x_{crit}, for water in Table 1 are used to represent data for dryout incipience quality, x_{di}, in the

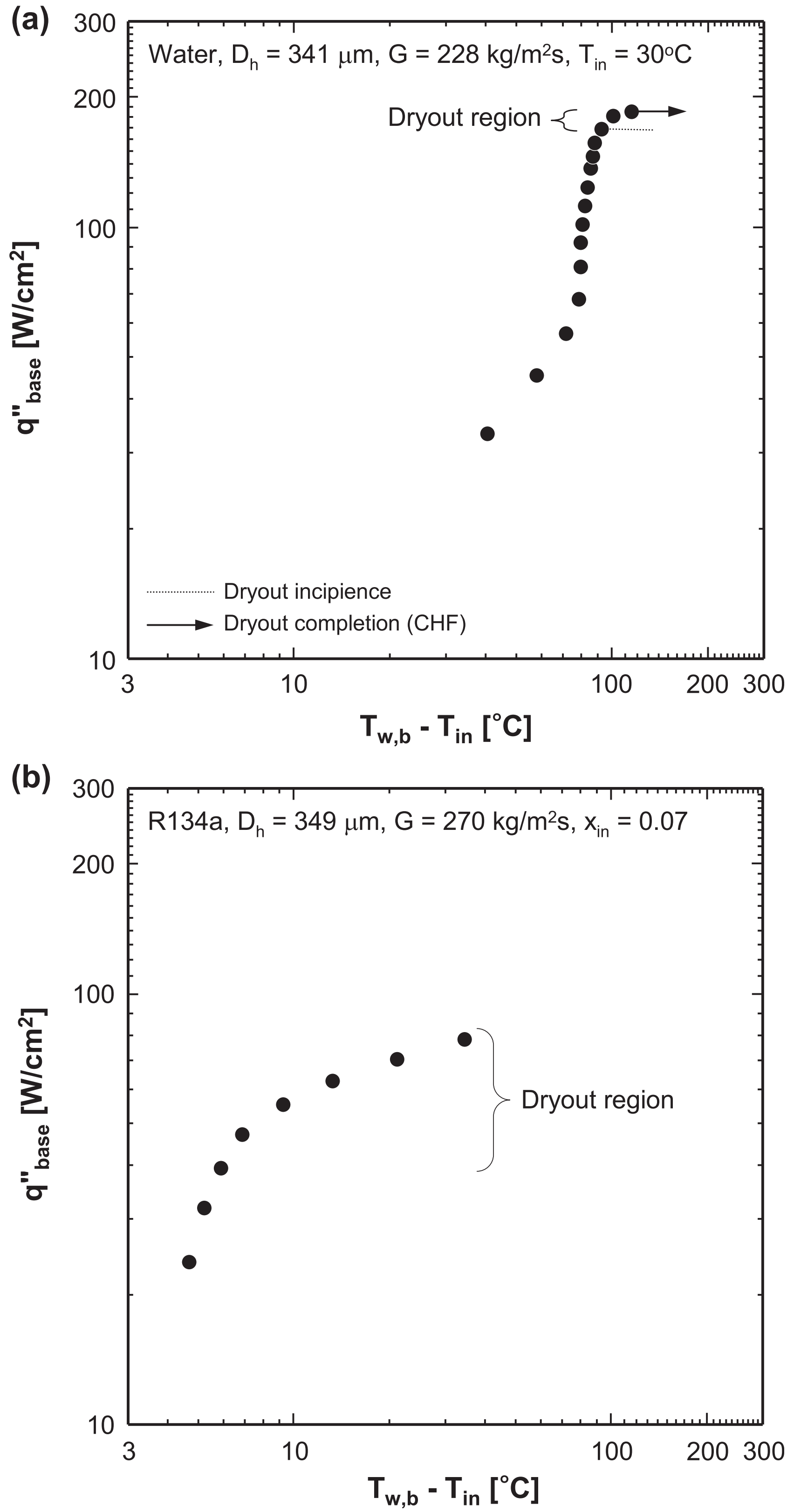

Fig. 2. Boiling curves for (a) water [41] and (b) R134a [42] flows in rectangular micro-channels.

development of the present correlation for dryout incipience quality.

Among the 333 dryout incipience quality data for fluids other than water, 203 data points were reported by the original authors, and 130 data points are identified by the present authors by the falling off in measured two-phase heat transfer coefficient attributed by the original authors to dryout incipience. For fluids other than water, the large differences between x_{di} and x_{crit} (as shown in Fig. 2(b)) necessitate accurate determination of x_{di} values.

Table 1
Consolidated database for saturated boiling mini/micro-channel flows used to develop present dryout incipience quality correlation.

Author(s)	Channel geometry[a]	Channel material	D_h [mm]	Relative roughness, e/D_h	Fluid(s)	G [kg/m^2 s]	Data points	Remarks[b]
Becker (1970) [44]	C, single, VU	–	2.4, 3.0	–	Water	365–2725	82	x_{crit} identified by fast increase of T_w
Lezzi et al. (1994) [45]	C, single, H	Stainless steel	1.0	Smooth	Water	776–2738	68	x_{crit} identified by fast increase of T_w of 5 °C
Baek and Chang (1997) [46]	C, single, VU	Stainless steel	6.0	–	Water	29–277	232	x_{crit} identified by fast increase of T_w when $T_w > 250$ °C
Roach et al. (1999) [47]	C, single, H	Copper	1.168, 1.448	0.0017, 0.0014	Water	256–1037	42	x_{crit} identified by fast increase of T_w when $T_w > 250$ °C
Kim et al. (2000) [48]	C, single, VU	Inconel-625	6.0	–	Water	99–277	210	x_{crit} identified by fast increase of T_w with T_w increase rate of 50 °C/s
Yang and Fujita (2002) [49]	R, single, H	Copper bottom, Pyrex cover	0.976	–	R113	100, 200	3	x^*_{di} identified by falling off of h_{tp}
Yu et al. (2002) [50]	C, single, H	Stainless steel	2.98	–	Water	50–151	30	x_{crit} identified by fast increase of T_w
Saitoh et al. (2005) [51]	C, single, H	Stainless steel	0.51, 1.12, 3.1	Smooth	R134a	150–300	41	x^*_{di} identified by falling off of h_{tp}
Yun et al. (2005) [34]	R, multi, H	Stainless steel	1.14	–	CO_2	300, 400	2	x^*_{di} identified by falling off of h_{tp}
Hihara and Dang (2007) [52]	C, single, H	Stainless steel	1.0, 2.0, 4.0, 6.0	Smooth	CO_2	360–1440	16	x_{di} identified by falling off of h_{tp}
Greco (2008) [53]	C, single, H	Stainless steel	6.0	Smooth	R134a, R22, R407C, R410A	199–1079	7	x^*_{di} identified by falling off of h_{tp}
Shiferaw (2008) [54]	C, single, VU	Stainless steel	1.1, 2.88, 4.26	0.0012, 0.0005, 0.0004	R134a	200–400	13	x^*_{di} identified by falling off of h_{tp}
Ohta et al. (2009) [55]	C, single, H	Stainless steel	0.51	–	FC72	107, 215	2	x^*_{di} identified by falling off of h_{tp}
Wang et al. (2009) [35]	C, single, H	Stainless steel	1.3	–	R134a	321–676	9	x^*_{di} identified by falling off of h_{tp}
Martín-Callizo (2010) [36]	C, single, VU	Stainless steel	0.64	0.0012	R134a, R22, R245fa	185–541	42	x_{di} identified by change of slope in boiling curve, and wall temperature fluctuation from $T_{w,std}$
Ali and Palm (2011) [40]	C, single, VU	Stainless steel	1.22, 1.70	0.0021, 0.0001	R134a	50–600	23	x_{di} identified by change of slope in boiling curve, and wall temperature fluctuation from $T_{w,std}$
Ducoulombier (2011) [56]	C, single, H	Stainless steel	0.529	0.0015–0.0030	CO_2	200–1410	48	x_{di} identified by falling off of h_{tp}
Oh and Son (2011a) [37]	C, single, H	Copper	1.77, 3.36, 5.35	Smooth	R134a, R22	200–400	6	x^*_{di} identified by falling off of h_{tp}
Oh and Son (2011b) [57]	C, single, H	Stainless steel	4.57	Smooth	CO_2	600–900	8	x^*_{di} identified by falling off of h_{tp}
Oh et al. (2011) [58]	C, single, H	Stainless steel	1.5, 3.0	Smooth	R22, R410A, R290	100–500	9	x^*_{di} identified by falling off of h_{tp}
Wu et al. (2011) [38]	C, single, H	Stainless steel	1.42	–	CO_2	300–600	18	x^*_{di} identified by falling off of h_{tp}
Del Col and Bortolin (2012) [59]	C, single, H	Copper	0.96	0.0014	R134a, R245fa, R32	101–902	43	x_{di} identified by wall temperature fluctuation from $T_{w,std}$
Karayiannis et al. (2012) [60]	C, single, VU	Stainless steel	1.1	0.0012	R134a	300	3	x_{di} identified by falling off of h_{tp}
Li et al. (2012) [39]	C, single, H	Stainless steel	2.0	Smooth	R1234yf, R32	100–400	8	x^*_{di} identified by falling off of h_{tp}
Mastrullo et al. (2012) [61]	C, single, H	Stainless steel	6.0	$\leqslant$0.00007	CO_2, R410A	150–501	28	x_{di} identified by falling off of h_{tp}
Tibiriçá et al. (2012) [62]	C. single, H	Stainless steel	1.0	0.0006	R1234ze	300–600	4	x^*_{di} identified by falling off of h_{tp}
Total							997	

[a] C: circular, R: rectangular, H: horizontal, VU: vertical upward.
[b] x_{crit}: critical quality data reported by original authors, x_{di}: dryout incipience quality data reported by original authors, x^*_{di}: dryout incipience quality data identified by present authors by falling off in measured two-phase heat transfer coefficient attributed by original authors to dryout incipience.

Data having a broad range of relative roughness are included in the consolidated database since the surface roughness ranges indicated in Table 1 where deemed to have minimal influence on dryout incipience quality. For the database of Ohta et al. [55], data points exhibiting flow rate fluctuations at the test section inlet are excluded from the consolidated database. For the data of Del Col and Bortolin [59], average heat flux values are used to represent non-uniformly heated micro-channels.

Table 2
Previous correlations for dryout incipience quality.

Author(s)	Equation	Remarks
Sun (2001) [63]	$x_{crit} = 10.795(q''_H/1000)^{-0.125} G^{-0.333} (1000D_h)^{-0.07} \exp\left(0.01715\times10^{-5}P\right)$ for $4.9bar \leqslant P \leqslant 29.4bar$,, $x_{crit} = 19.398(q''_H/1000)^{-0.125} G^{-0.333} (1000D_h)^{-0.07} \exp\left(-0.00255\times10^{-5}P\right)$ for $29.4bar \leqslant P \leqslant 98bar$, $x_{crit} = 32.302(q''_H/1000)^{-0.125} G^{-0.333} (1000D_h)^{-0.07} \exp\left(-0.00795\times10^{-5}P\right)$ for $98bar \leqslant P \leqslant 196bar$, $Fr^* = \frac{x_{crit}G}{\sqrt{\rho_g(\rho_f-\rho_g)g\cos\theta D_h}}$, $\theta = 0$ for horizontal flow, $x_{di} = x_{crit} - \frac{8}{(2+Fr^*)^2}$, q''_H in [W/m^2], G in [kg/m^2 s], D_h in [m], P in [Pa]	D = 4.572 mm, CO_2
Yoon et al. (2004) [64]	$x_{di} = 0.0012 Re_{fo}^{2.79}(1000Bo)^{0.06}Bd^{-4.76}$, $Re_{fo} = \frac{GD_h}{\mu_f}, Bo = \frac{q''_H}{Gh_{fg}}, Bd = \frac{g(\rho_f-\rho_g)D_h^2}{\sigma}$	D = 7.53 mm, CO_2
Wojtan et al. (2005) [65]	$x_{di} = 0.58exp\left[0.52 - 0.235 We_g^{0.17} Fr_{g,Mori}^{0.37}\left(\frac{\rho_g}{\rho_f}\right)^{0.25}\left(\frac{q''_H}{q''_{crit}}\right)^{0.70}\right]$, $We_g = \frac{G^2D_{eq}}{\rho_g\sigma}, Fr_{g,Mori} = \frac{G^2}{\rho_g(\rho_f-\rho_g)gD_{eq}}, D_{eq} = \sqrt{\frac{4A}{\pi}}$, $q''_{crit} = 0.131\rho_g^{0.5}h_{fg}\left[g\sigma(\rho_f-\rho_g)\right]^{0.25}$	D = 8.00, 13.84 mm, R22, R410A
Cheng et al. (2006) [66]	$x_{di} = 0.58exp\left[0.52 - 0.67 We_g^{0.17} Fr_{g,Mori}^{0.348}\left(\frac{\rho_g}{\rho_f}\right)^{0.25}\left(\frac{q''_H}{q''_{crit}}\right)^{0.70}\right]$	D_h = 0.8–10.06 mm, CO_2
Del Col et al. (2007) [67]	$x_{di} = 0.4695\left(\frac{4q''_H\cdot RLL}{GD_hh_{fg}}\right)^{1.472}\left(\frac{G^2D_h}{\rho_f\sigma}\right)^{0.3024}\left(\frac{D_h}{0.001}\right)^{0.1836}(1-P_R)^{1.239}$, $RLL = \left[0.437\left(\frac{\rho_g}{\rho_f}\right)^{0.073}\left(\frac{\rho_f\sigma}{G^2}\right)^{0.24}D_h^{0.72}\left(\frac{Gh_{fg}}{q''_H}\right)\right]^{1/0.96}$, D_h in [m]	Mini-channels, refrigerants, CO_2
Cheng et al. (2008) [68]	$x_{di} = 0.58exp\left[0.52 - 0.236 We_g^{0.17} Fr_{g,Mori}^{0.17}\left(\frac{\rho_g}{\rho_f}\right)^{0.25}\left(\frac{q''_H}{q''_{crit}}\right)^{0.27}\right]$	D_h = 0.6–10.06 mm, CO_2
Jeong and Park (2009) [69]	$x_{di} = 6.2Re_{fo}^{-0.5}Bo^{-0.2}Bd^{-0.45}$	D = 0.80, 0.81 mm, CO_2
Ducoulombier et al. (2011) [56]	$x_{di} = 1 - 338Bo^{0.703}P_R^{1.43}$	D = 0.529 mm, CO_2
Mastrullo et al. (2012) [61]	$x_{di} = 1 - 20.82q''^{0.273}_H G^{1.231} D_h^{0.252}\frac{\mu_f}{h_{fg}^{0.273}(\rho_f\sigma)^{1.252}}P_R^{-0.721}$, q''_H in [W/m^2], G in [kg/m^2 s], D_h in [m]	D = 6.00 mm, R410A, CO_2

The consolidated database covers a broad range of reduced pressures, from 0.005 to 0.78. The high pressure data include those of Yun et al. [34], P_R = 0.54, Hihara and Dang [52], P_R = 0.69, Ducoulombier et al. [56], P_R = 0.36–0.47, Oh and Son [57], P_R = 0.61–0.78, Wu et al. [38], P_R = 0.14–0.47, and Mastrullo et al. [61], P_R = 0.30–0.64.

In all, the consolidated database includes 997 dryout incipience quality and dryout completion quality (CHF) data points with the following coverage:

– Working fluid: FC72, R113, R1234yf, R1234ze, R134a, R22, R245fa, R290, R32, R407C, R410A, CO_2, and water.

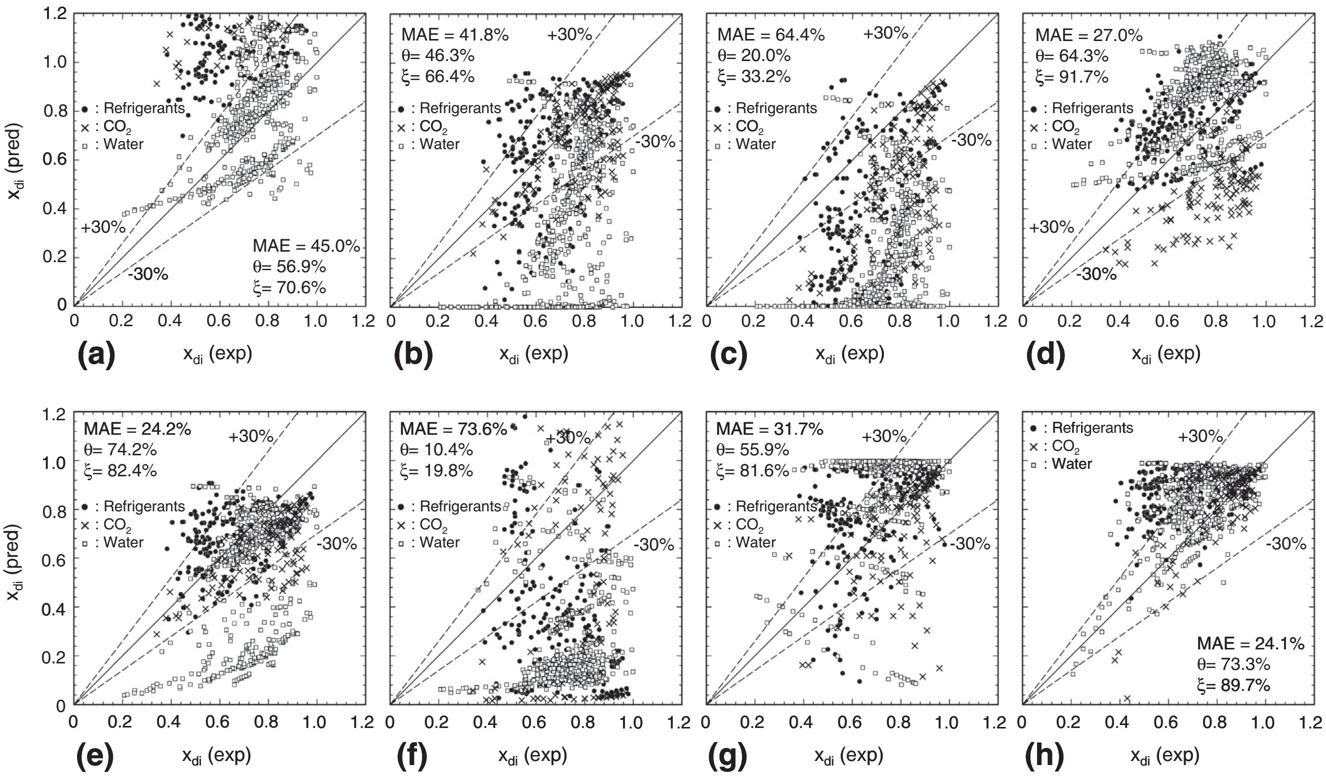

Fig. 3. Comparison of consolidated 997 point database with predictions of previous correlations: (a) Sun (2001) [63], (b) Wojtan et al. (2005) [65], (c) Cheng et al. (2006) [66], (d) Del Col et al. (2007) [67], (e) Cheng et al. (2008) [68], (f) Jeong and Park (2009) [69], (g) Ducoulombier et al. (2011) [56], and (h) Mastrullo et al. (2012) [61].

– Hydraulic diameter: $0.51 < D_h < 6.0$ mm.
– Mass velocity: $29 < G < 2303$ kg/m^2 s.
– Liquid-only Reynolds number: $125 < Re_{fo} = GD_h/\mu_f < 53{,}770$.
– Boiling number: $0.31 \times 10^{-4} < Bo = q''_H/Gh_{fg} < 44.3 \times 10^{-4}$.
– Reduced pressure: $0.005 < P_R < 0.78$.

3. Evaluation of previous correlations

Three different parameters are used to assess the accuracy of individual correlations. θ and ξ are defined as the percentages of predictions within ±30% and ±50%, respectively, of the data, and MAE is the mean absolute error, which is defined as

$$\mathrm{MAE} = \frac{1}{N}\sum \frac{|x_{di,pred} - x_{di,exp}|}{x_{di,exp}} \times 100\% \tag{1}$$

When comparing the consolidated database to predictions of previous models or correlations, thermophysical properties are obtained using NIST's REFPROP 8.0 software [70], excepting those for FC-72, which are obtained from 3M Company.

Table 3
New dryout incipience quality correlation for saturated boiling mini/micro-channel flows.

$x_{di} = 1.4 We_{fo}^{0.03} P_R^{0.08} - 15.0 \left(Bo \frac{P_H}{P_F}\right)^{0.15} Ca^{0.35} \left(\frac{\rho_g}{\rho_f}\right)^{0.06}$
where $We_{fo} = \frac{G^2 D_h}{\rho_f \sigma}$, $P_R = \frac{P}{P_{crit}}$, $Bo = \frac{q''_H}{G h_{fg}}$, $Ca = \frac{\mu_f G}{\rho_f \sigma} = \frac{We_{fo}}{Re_{fo}}$,
q''_H: effective heat flux averaged over heated perimeter of channel,
P_H: heated perimeter of channel, P_F: wetted perimeter of channel

Table 2 provides a summary of previous dryout incipience quality, x_{di}, correlations. It should be emphasized that each of these correlations was derived for specific fluids and limited ranges of operating conditions. Notice that the correlations of Cheng et al. [66,68], Del Col et al. [67], Jeong and Park [69], and Ducoulombier et al. [56] were developed specifically for mini/micro-channel flows. The correlation of Sun [63] was based on equations

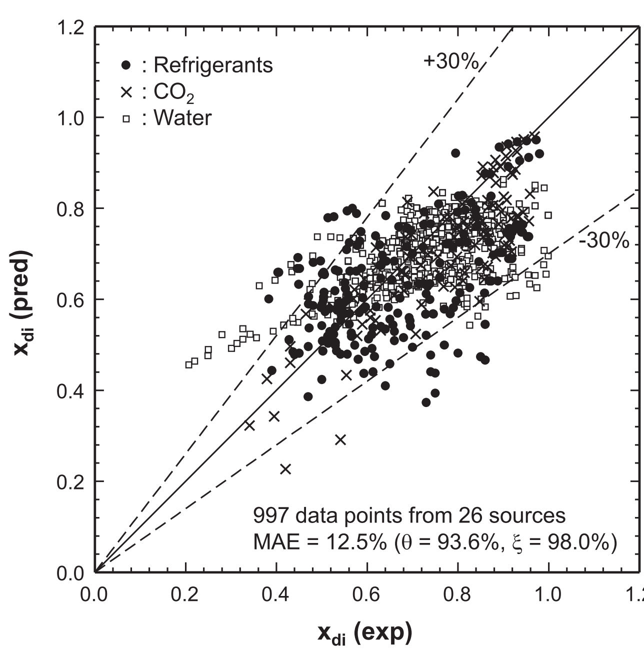

Fig. 4. Comparison of predictions of new correlation with 997 point consolidated database.

developed by Kon'kov [71] for water upward through vertical tubes. The correlation of Wojtan et al. [65] was based on a functional formulation by Mori et al. [72], and the correlations of Cheng et al. [66,68] are modified versions of those of Wojtan et al. [65] tailored specially to CO_2 flows. The correlation of Jeong and Park [69] was based on a functional formulation by Yoon et al. [64]. The relatively simple correlation of Ducoulombier et al. [56] was developed specifically for lower saturation temperatures and lower heat fluxes.

Fig. 3 compares the entire 997-point consolidated database for mini/micro-channel flows with predictions of previous correlations for dryout incipience quality, x_{di}. Given the large differences in thermophysical properties for different working fluids, the 13 fluids are segregated into three categories: refrigerants, CO_2, and water. The correlation of Yoon et al. [64] is excluded from this comparison because of its unusually high MAE and significant scatter. Fig. 3(a) shows the correlation of Sun [63] highly overpredicts most of the consolidated database except for water data. Large portions of the consolidated database are highly underpredicted by the correlations of Wojtan et al. [65], Fig. 3(b), Cheng et al. [66], Fig. 3(c), and Jeong and Park [69], Fig. 3(f). As shown in Fig. 3(d), the correlation of Del Col et al. [67] displays some scatter against the consolidated database, and significant underprediction of CO_2 data. Excluding water data, the correlation of Cheng et al. [68] provides fair predictions, Fig. 3(e), married by some overprediction of refrigerant data and some underprediction of CO_2 data. The correlation of Ducoulombier et al. [12] shows large scatter against most of the consolidated database, especially for refrigerants and water. Interestingly, the correlation of Mastrullo et al. [61], which was developed for refrigerants and CO_2 flows in 6-mm diameter circular tubes, shows better MAE than all other seven correlations, despite some overprediction of the data.

4. New generalized correlation

Various combinations of dimensional parameters are examined in the development of a generalized correlation for dryout incipience quality. The relative influences of inertia, viscous force, and surface tension, are accounted for using the Weber and Capillary numbers, which are defined as

$$We_{fo} = \frac{G^2 D_h}{\rho_f \sigma} \tag{2}$$

and

$$Ca = \frac{\mu_f G}{\rho_f \sigma} = \frac{We_{fo}}{Re_{fo}} \tag{3}$$

respectively. Both reduced pressure, $P_R (= P/P_{crit})$, and density ratio, ρ_f/ρ_g, are also considered to cope with different working fluids, such as refrigerants, CO_2, and water, and broad variations in operating pressure. The effect of heat flux is accounted for using the Boiling number, which is defined as

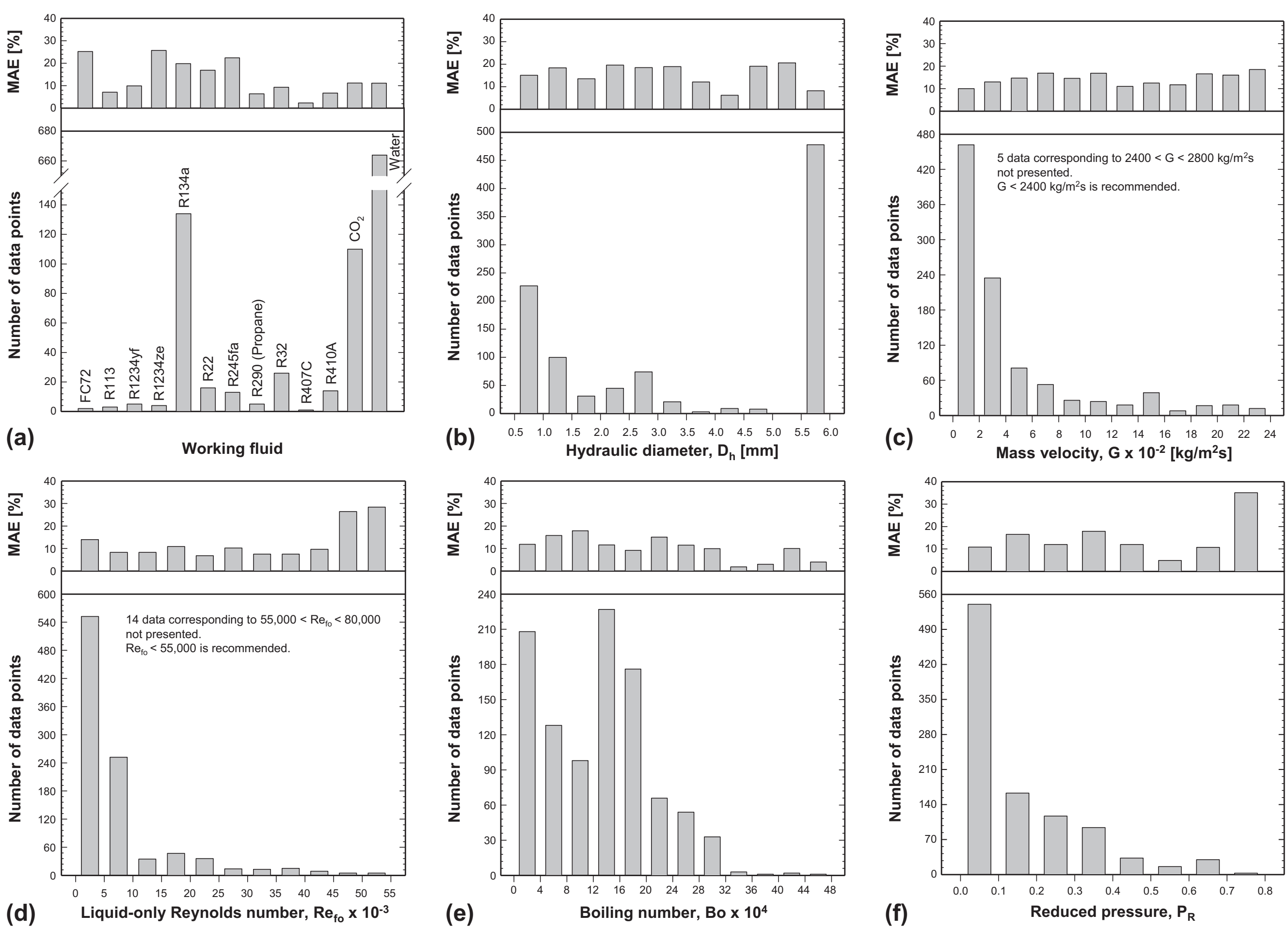

Fig. 5. Distributions of number of data points and MAE in predictions of new correlation for 997 point database relative to: (a) working fluid, (b) hydraulic diameter, (c) mass velocity, (d) liquid-only Reynolds number, (e) Boiling number, and (f) reduced pressure.

$$Bo = \frac{q''_H}{G h_{fg}} \quad (4)$$

where q''_H is the effective heat flux averaged over the heated perimeter of the channel. The ratio of the flow channel's heated to wetted perimeters, P_H/P_F, is also considered to cope with one-sided wall heating by Yang and Fujita [49]. Using the entire consolidated database for flow boiling in mini/micro-channels, the following correlation for dryout incipience quality is proposed,

$$x_{di} = 1.4 We_{fo}^{0.03} P_R^{0.08} - 15.0 \left(Bo \frac{P_H}{P_F} \right)^{0.15} Ca^{0.35} \left(\frac{\rho_g}{\rho_f} \right)^{0.06} \quad (5)$$

whose empirical constants are optimized to yield least MAE. Table 3 provides detailed definitions of this correlation's individual dimensionless parameters.

Fig. 4 shows the new dryout incipience quality correlation predicts the 997-point consolidated mini/micro-channel flow boiling database with good accuracy, evidenced by a MAE of 12.5%, with 93.6% and 98.0% of the data falling within ±30% and ±50% error bands, respectively.

But achieving low overall MAE is by no means the only definitive means for ascertaining the effectiveness of the new correlation. Equally crucial is the ability of the correlation to predict data evenly over relatively broad ranges of all relevant parameters [19-21,23,24].

Fig. 5 shows, for each parameter, both a lower bar chart distribution of number of data points, and corresponding upper bar chart distribution of MAE in the predictions of the new correlation. The 997-point consolidated database is segregated into different working fluids and narrow bins of hydraulic diameter, D_h, mass velocity, G, liquid-only Reynolds number, Re_{fo}, Boiling number, Bo, and reduced pressure, P_R. The new correlation shows very good predictions for most parameter bins, evidenced by MAE values mostly below 20%.

Another measure of the accuracy of the new correlation is the ability to yield evenly good predictions for individual databases comprising the consolidated database. Table 4 compares individual mini/micro-channel databases from 26 sources with predictions of the present correlation as well as select previous correlations that have shown relatively superior predictive capability as discussed earlier. The present correlation provides good predictions for all individual databases with MAE values mostly around 10% and 11 databases predicted more accurately than by any of the select previous correlations. The new correlation also possesses the best overall MAE of 12.5%.

Fig. 6 shows an assessment of the accuracy and limitations of the select previous correlations against hydraulic diameter. Notice that the correlations of Wojtan et al. [65] and Cheng et al. [68]

Table 4
Comparison of individual mini/micro-channel dryout incipience databases with predictions of select previous correlations and present correlation.

Author(s)	D_h [mm]	Fluid(s)	Mean absolute error (%)				
			Wojtan et al. (2005) [65]	Del Col et al. (2007) [67]	Cheng et al. (2008) [68]	Mastrullo et al. (2012) [61]	New correlation
Becker (1970)[44]	2.4, 3.0	Water	96.3	24.2	69.0	10.2	19.8
Lezzi et al. (1994) [45]	1.0	Water	95.9	26.5	71.8	8.6	9.4
Baek and Chang (1997) [46]	6.0	Water	36.6	25.8	9.9	21.8	9.2
Roach et al. (1999) [47]	1.168, 1.448	Water	94.8	23.1	45.3	32.0	22.5
Kim et al. (2000) [48]	6.0	Water	29.1	28.5	8.7	24.2	7.2
Yang and Fujita (2002) [49]	0.976	R113	15.5	33.4	26.5	37.5	7.1
Yu et al. (2002) [50]	2.98	Water	30.8	33.2	25.4	31.7	19.6
Saitoh et al. (2005) [51]	0.51, 1.12, 3.1	R134a	23.1	17.9	26.0	29.2	22.1
Yun et al. (2005) [34]	1.14	CO_2	19.2	40.1	3.5	33.1	6.1
Hihara and Dang (2007) [52]	1.0, 2.0, 4.0, 6.0	CO_2	8.8	56.2	15.4	35.5	12.8
Greco (2008) [53]	6.0	R134a, R22, R407C, R410A	12.8	33.9	11.3	11.5	14.7
Shiferaw (2008) [54]	1.1, 2.88, 4.26	R134a	18.1	39.8	19.3	52.7	7.6
Ohta et al. (2009) [55]	0.51	FC72	17.9	16.4	20.9	32.5	25.2
Wang et al. (2009) [35]	1.3	R134a	19.1	3.5	13.3	13.0	16.6
Martín-Callizo (2010) [36]	0.64	R134a, R22, R245fa	29.4	24.9	25.9	61.3	16.5
Ali and Palm (2011) [40]	1.22, 1.70	R134a	40.5	38.1	31.1	54.1	22.0
Ducoulombier (2011) [56]	0.529	CO_2	24.3	38.1	24.0	18.0	13.4
Oh and Son (2011a) [37]	1.77, 3.36, 5.35	R134a, R22	5.6	10.6	12.2	6.5	11.1
Oh and Son (2011b) [57]	4.57	CO_2	13.6	51.2	21.2	50.2	19.1
Oh et al. (2011) [58]	1.5, 3.0	R22, R410A, R290	19.1	29.6	12.8	33.4	13.5
Wu et al. (2011) [38]	1.42	CO_2	6.0	20.2	13.8	8.6	5.8
Del Col and Bortolin (2012) [59]	0.96	R134a, R245fa, R32	45.4	10.5	17.0	31.7	20.1
Karayiannis et al. (2012) [60]	1.1	R134a	9.7	22.7	15.8	38.7	9.5
Li et al. (2012) [39]	2.0	R1234yf, R32	8.5	5.8	5.2	14.2	8.8
Mastrullo et al. (2012) [61]	6.0	CO_2, R410A	2.0	40.5	14.2	2.1	5.2
Tibiriçá et al. (2012) [62]	1.0	R1234ze	32.6	10.3	22.7	5.6	25.7
Total			41.8	27.0	24.2	24.1	12.5

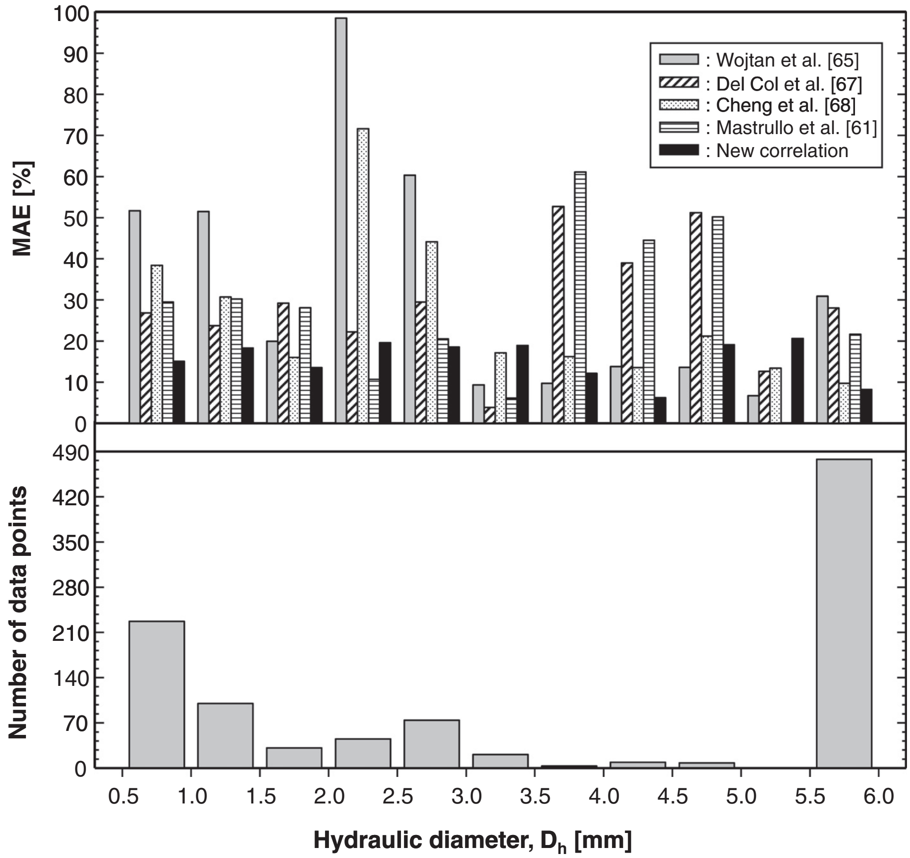

Fig. 6. Distribution of MAE in predictions of select previous correlations and present correlation for entire 997 point database relative to hydraulic diameter.

provide inferior predictions for most diameters below 3 mm. On the other hand, the correlations of Del Col et al. [67] and Mastrullo et al. [61] provide inferior predictions for most diameters above 3 mm. In contrast, the predictive accuracy of the new correlation is not compromised for different diameter bins.

To further explore the accuracy of the present correlation, the effects of different working fluids are examined. Table 5 shows predictions of the present and previous correlations compared to three subsets of the consolidated database: refrigerants, CO_2, and water. Notice that, while some of the previous correlations do provide fair predictions for one fluid subset, they generally show poor predictions for other fluid subsets. On the other hand, the new correlation shows the best predictions for all three data subsets, evidenced by MAEs of 17.1% for refrigerants, 11.2% for CO_2, and 11.2% for water.

Fig. 7(a)–(d) shows a parametric assessment of the effects of working fluid, heat flux, channel diameter, and saturation pressure, respectively, on dryout incipience quality using the new correlation. Fig. 7(a) shows the predicted dryout incipience quality decreases with increasing mass velocity for FC72, R134a, and CO_2, whereas, for water, it increases with increasing mass velocity. Notice in Fig. 7(b) the change in the trend of G vs. x_{di} with increasing heat flux for water: x_{di} increases with increasing G for low heat fluxes but decreases for high heat fluxes. In the same figure, the trend of G vs. x_{di} for R134a is monotonic regardless of heat flux. Fig. 7(c) shows the dryout incipience quality increases with

Table 5
Assessment of previous correlations and present correlation against consolidated database for refrigerants, CO_2, and water[a].

Author(s)	Refrigerants dryout incipience database (223 points)			CO_2 dryout incipience database (110 points)			Water dryout incipience database (664 points)		
	MAE (%)	θ (%)	ξ (%)	MAE (%)	θ (%)	ξ (%)	MAE (%)	θ (%)	ξ (%)
Sun (2001) [63]	85.2	20.6	32.7	128.6	0.9	10.0	22.7	78.5	92.9
Yoon et al. (2004) [64]	–	2.2	2.2	–	1.8	4.5	–	0	0
Wojtan et al. (2005) [65]	27.3	63.7	81.2	14.6	80.9	98.2	51.1	34.8	56.2
Cheng et al. (2006) [66]	44.8	39.5	62.3	40.4	44.5	62.7	75.0	9.3	18.5
Del Col et al. (2007) [67]	21.3	74.9	92.8	40.8	20.0	73.6	26.7	68.1	94.3
Cheng et al. (2008) [68]	21.0	79.4	93.7	18.9	80.9	100	26.1	71.4	75.8
Jeong and Park (2009) [69]	85.3	16.1	36.3	57.3	30.9	40.9	72.3	5.1	10.7
Ducoulombier et al. (2011) [56]	32.5	54.7	75.8	22.0	74.5	83.6	33.0	53.2	83.3
Mastrullo et al. (2012) [61]	36.1	50.2	66.4	19.0	80.0	95.5	20.9	80.0	96.6
New correlation	17.1	87.9	97.8	11.2	98.2	100	11.2	94.7	97.7

[a] Dash indicates mean absolute error ≫ 100%.

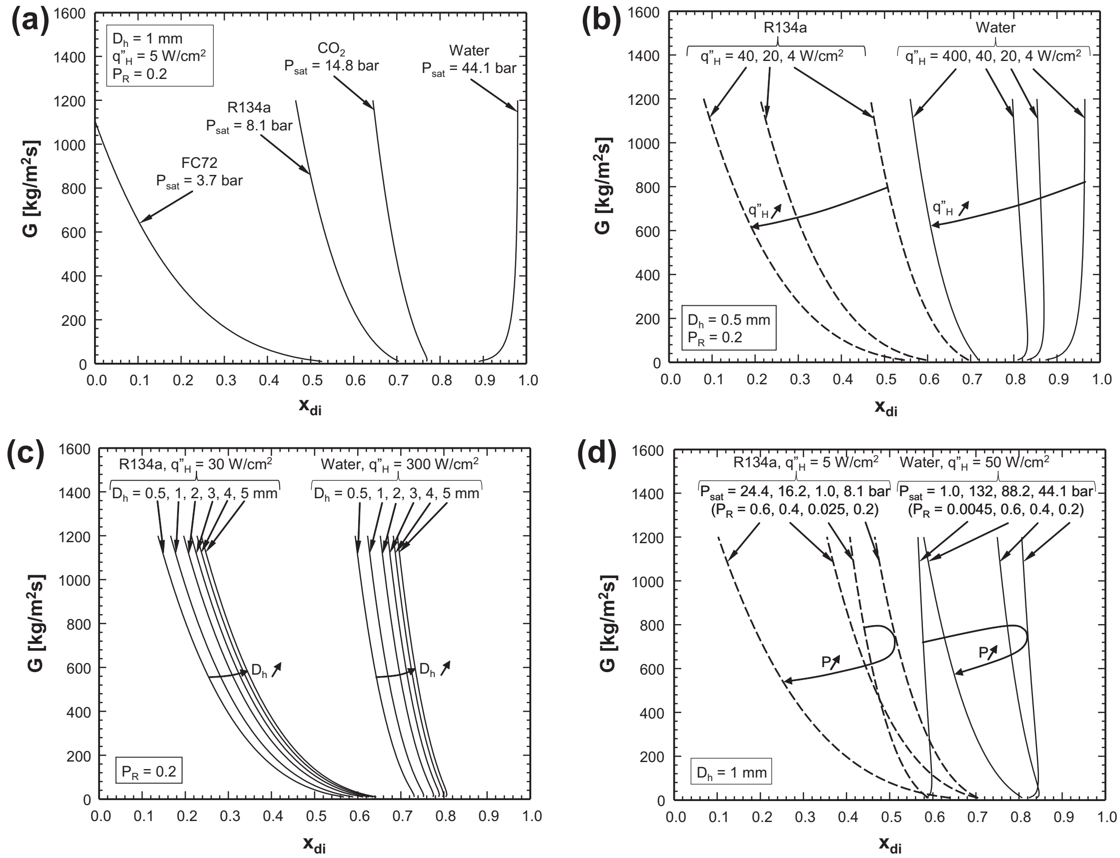

Fig. 7. Effects of (a) working fluid, (b) heat flux, (c) channel diameter, and (d) saturation pressure on predictions of present dryout incipience quality correlation.

increasing diameter. Fig. 7(d) shows the influence of reduced pressure is not monotonic because of the strong dependence of thermophysical properties in the individual dimensionless parameters of the new correlation on saturation pressure. For both R134a and water, Fig. 7(d) shows x_{di} increasing with increasing saturation pressure up to P_R = 0.2 and decreasing for higher pressures.

5. Conclusions

This two-part study examines the development of a generalized approach to predicting heat transfer for flow boiling in mini/micro-channel flows. Boiling heat transfer in small channels is either Nucleate Boiling dominated or Convective Boiling dominated, and the generalized approach must be able to tackle both heat transfer regimes. However, both regimes exhibit substantial reduction in the heat transfer coefficient where partial dryout commences in the annular liquid film, and this occurs upstream of the complete film dryout associated with CHF. Therefore, a systematic generalized heat transfer correlation must address both the Nucleate Boiling dominated and Convective Boiling dominated regimes only up to the location of incipient dryout because of the drastic changes in heat transfer behavior that occur downstream of this location. This points to the need for determining the occurrence of this important transition point. This first part of the study concerns the development of a correlation for dryout incidence quality. This goal is accomplished by first amassing a consolidated database consisting of 997 dryout incipience quality and dryout completion quality data points for 13 fluids from 26 sources. Key findings from the study are as follows:

(1) Comparing the consolidated database with predictions of previous dryout incipience correlations shows poor results for certain fluids. By segregating data into three fluid subsets of water, CO_2 and refrigerants, it is shown that some of the prior correlations provide fair predictions for one or two fluid subsets, and poor predictions for the other(s).
(2) A generalized correlation is proposed for dryout incipience quality in mini/micro-channel flows. This correlation shows excellent predictive capability against the entire consolidated database, with an overall MAE of 12.5%, and 93.6% and 98.0% of the predictions falling within ±30% and ±50% of the data, respectively. The predictive accuracy of the new correlation is also fairly even for the 13 different working fluids, and over broad ranges of all relevant parameters.

Acknowledgment

The authors are grateful for the partial support for this project from the National Aeronautics and Space Administration (NASA) under Grant no. NNX13AC83G.

References

[1] T.M. Anderson, I. Mudawar, Microelectronic cooling by enhanced pool boiling of a dielectric fluorocarbon liquid, J. Heat Transfer – Trans. ASME 111 (1989) 752–759.
[2] I. Mudawar, A.H. Howard, C.O. Gersey, An analytical model for near-saturated pool boiling CHF on vertical surfaces, Int. J. Heat Mass Transfer 40 (1997) 2327–2339.

[3] T.C. Willingham, I. Mudawar, Forced-convection boiling and critical heat flux from a linear array of discrete heat sources, Int. J. Heat Mass Transfer 35 (1992) 2879–2890.

[4] T.N. Tran, M.W. Wambsganss, D.M. France, Small circular- and rectangular-channel boiling with two refrigerants, Int. J. Multiphase Flow 22 (1996) 485–498.

[5] H.J. Lee, S.Y. Lee, Heat transfer correlation for boiling flows in small rectangular horizontal channels with low aspect ratios, Int. J. Multiphase Flow 27 (2001) 2043–2062.

[6] Y. Katto, M. Kunihiro, Study of the mechanism of burn-out in boiling system of high burn-out heat flux, Bull. JSME 16 (1973) 1357–1366.

[7] M. Monde, T. Inoue, Critical heat flux in saturated forced convective boiling on a heated disk with multiple impinging jets, J. Heat Transfer – Trans. ASME 113 (1991) 722–727.

[8] D.C. Wadsworth, I. Mudawar, Enhancement of single-phase heat transfer and critical heat flux from an ultra-high-flux-source to a rectangular impinging jet of dielectric liquid, J. Heat Transfer – Trans. ASME 114 (1992) 764–768.

[9] M.E. Johns, I. Mudawar, An ultra-high power two-phase jet-impingement avionic clamshell module, J. Electron. Packag. – Trans. ASME 118 (1996) 264–270.

[10] S. Toda, A study in mist cooling (1st report: investigation of mist cooling), Trans. JSME 38 (1972) (1972) 581–588.

[11] L. Lin, R. Ponnappan, Heat transfer characteristics of spray cooling in a closed loop, Int. J. Heat Mass Transfer 46 (2003) 3737–3746.

[12] J.R. Rybicki, I. Mudawar, Single-phase and two-phase cooling characteristics of upward-facing and downward-facing sprays, Int. J. Heat Mass Transfer 49 (2006) 5–16.

[13] M. Visaria, I. Mudawar, Theoretical and experimental study of the effects of spray orientation on two-phase spray cooling and critical heat flux, Int. J. Heat Mass Transfer 51 (2008) 2398–2410.

[14] W. Nakayama, T. Nakajima, S. Hirasawa, Heat sink studs having enhanced boiling surfaces for cooling of microelectronic components, ASME Paper 84-WA/HT-89, 1984.

[15] R.L. Webb, The evolution of enhanced surface geometries for nucleate boiling, Heat Transfer Eng. 2 (1981) 46–69.

[16] V. Khanikar, I. Mudawar, T. Fisher, Effects of carbon nanotube coating on flow boiling in a micro-channel, Int. J. Heat Mass Transfer 52 (2009) 3805–3817.

[17] M.K. Sung, I. Mudawar, Experimental and numerical investigation of single-phase heat transfer using a hybrid jet-impingement/micro-channel cooling scheme, Int. J. Heat Mass Transfer 49 (2006) 682–694.

[18] M.K. Sung, I. Mudawar, Correlation of critical heat flux in hybrid jet impingement/micro-channel cooling scheme, Int. J. Heat Mass Transfer 49 (2006) 2663–2672.

[19] S.M. Kim, I. Mudawar, Universal approach to predicting two-phase frictional pressure drop for adiabatic and condensing mini/micro-channel flows, Int. J. Heat Mass Transfer 55 (2012) 3246–3261.

[20] S.M. Kim, I. Mudawar, Universal approach to predicting two-phase frictional pressure drop for mini/micro-channel saturated flow boiling, Int. J. Heat Mass Transfer 58 (2013) 718–734.

[21] S.M. Kim, I. Mudawar, Universal approach to predicting heat transfer coefficient for condensing mini/micro-channel flows, Int. J. Heat Mass Transfer 56 (2013) 238–250.

[22] D.D. Hall, I. Mudawar, Ultra-high critical heat flux (CHF) for subcooled water flow boiling – II. High-CHF database and design parameters, Int. J. Heat Mass Transfer 42 (1999) 1429–1456.

[23] D.D. Hall, I. Mudawar, Critical heat flux (CHF) for water flow in tubes – I. Compilation and assessment of world CHF data, Int. J. Heat Mass Transfer 43 (2000) 2573–2604.

[24] D.D. Hall, I. Mudawar, Critical heat flux (CHF) for water flow in tubes – II. Subcooled CHF correlations, Int. J. Heat Mass Transfer 43 (2000) 2605–2640.

[25] S.S. Kutateladze, A.I. Leont'ev, Some applications of the asymptotic theory of the turbulent boundary layer, in: Proc. 3rd Int. Heat Transfer Conf., Chicago, Illinois 3, 1966, pp. 1–6.

[26] L.S. Tong, Boundary-layer analysis of the flow boiling crisis, Int. J. Heat Mass Transfer 11 (1968) 1208–1211.

[27] W. Hebel, W. Detavernier, M. Decreton, A contribution to the hydrodynamics of boiling crisis in a forced flow of water, Nucl. Eng. Des. 64 (1981) 443–445.

[28] J. Weisman, B.S. Pei, Prediction of critical heat flux in flow boiling at low qualities, Int. J. Heat Mass Transfer 26 (1983) 1463–1477.

[29] C.H. Lee, I. Mudawar, A mechanistic critical heat flux model for subcooled flow boiling based on local bulk flow conditions, Int. J. Multiphase Flow 14 (1988) 711–728.

[30] C.O. Cersey, I. Mudawar, Effects of heater length and orientation on the trigger mechanism for near-saturated flow boiling critical heat flux – I. Photographic study and statistical characterization of the near-wall interfacial features, Int. J. Heat Mass Transfer 38 (1995) 629–641.

[31] C.O. Cersey, I. Mudawar, Effects of heater length and orientation on the trigger mechanism for near-saturated flow boiling critical heat flux – II. Critical heat flux model, Int. J. Heat Mass Transfer 38 (1995) 643–654.

[32] J.C. Sturgis, I. Mudawar, Critical heat flux in a long, rectangular channel subjected to one sided heating – I. Flow visualization, Int. J. Heat Mass Transfer 42 (1999) 1835–1847.

[33] J.C. Sturgis, I. Mudawar, Critical heat flux in a long, rectangular channel subjected to one sided heating – II. Analysis of critical heat flux data, Int. J. Heat Mass Transfer 42 (1999) 1849–1862.

[34] R. Yun, Y. Kim, M.S. Kim, Convective boiling heat transfer characteristics of CO_2 in microchannels, Int. J. Heat Mass Transfer 48 (2005) 235–242.

[35] L. Wang, M. Chen, M. Groll, Flow boiling heat transfer characteristics of R134a in a horizontal mini tube, J. Chem. Eng. Data 54 (2009) 2638–2645.

[36] C. Martín-Callizo, Flow boiling heat transfer in single vertical channel of small diameter, Ph.D. Thesis, Royal Institute of Technology, Sweden, 2010.

[37] H.K. Oh, C.H. Son, Evaporation flow pattern and heat transfer of R-22 and R-134a in small diameter tubes, Heat Mass Transfer 47 (2011) 703–717.

[38] J. Wu, T. Koettig, Ch. Franke, D. Helmer, T. Eisel, F. Haug, J. Bremer, Investigation of heat transfer and pressure drop of CO_2 two-phase flow in a horizontal minichannel, Int. J. Heat Mass Transfer 54 (2011) 2154–2162.

[39] M. Li, C. Dang, E. Hihara, Flow boiling heat transfer of HFO1234yf and R32 refrigerant mixtures in a smooth horizontal tube: part I. Experimental investigation, Int. J. Heat Mass Transfer 55 (2012) 3437–3446.

[40] R. Ali, B. Palm, Dryout characteristics during flow boiling of R134a in vertical circular minichannels, Int. J. Heat Mass Transfer 54 (2011) 2434–2445.

[41] W. Qu, I. Mudawar, Measurement and correlation of critical heat flux in two-phase micro-channel heat sinks, Int. J. Heat Mass Transfer 47 (2004) 2045–2059.

[42] J. Lee, I. Mudawar, Two-phase flow in high-heat-flux micro-channel heat sink for refrigeration cooling applications: part II – heat transfer characteristics, Int. J. Heat Mass Transfer 48 (2005) 941–955.

[43] S.M. Kim, I. Mudawar, Universal approach to predicting saturated flow boiling heat transfer in mini/micro-channels – Part II. Two-phase heat transfer coefficient, Int. J. Heat Mass Transfer, 2013. http://dx.doi.org/10.1016/j.ijheatmasstransfer.2013.04.014 .

[44] K.M. Becker, Burnout measurements in vertical round tubes, effect of diameter, AE-TPM-RL-1260, Aktiebolaget Atomenergi, 1970.

[45] A.M. Lezzi, A. Niro, G.P. Beretta, Experimental data on CHF for forced convection water boiling in long horizontal capillary tubes, in: Proc. 10th Int. Heat Transfer Conf., vol. 7, UK, 1994, pp. 491–496.

[46] W.P. Baek, S.H. Chang, KAIST CHF data, Personal communication, Korea Advanced Institute of Science and Technology, Taejon, South Korea, 8, 1997.

[47] G.M. Roach Jr., S.I. Abdel-Kahlik, S.M. Ghiaasiaan, M.F. Dowling, S.M. Jeter, Low-flow critical heat flux in heated microchannels, Nucl. Sci. Eng. 131 (1999) 411–425.

[48] H.C. Kim, W.P. Baek, S.H. Chang, Critical heat flux of water in vertical round tubes at low pressure and low flow conditions, Nucl. Eng. Des. 199 (2000) 49–73.

[49] Y. Yang, Y. Fujita, Boiling heat transfer in rectangular channels of small gaps, Memoirs of the Faculty of Engineering, Kyushu University, vol. 62, 2002, pp. 223–239.

[50] W. Yu, D.M. France, M.W. Wambsganss, J.R. Hull, Two-phase pressure drop, boiling heat transfer, and critical heat flux to water in a small-diameter horizontal tube, Int. J. Multiphase Flow 28 (2002) 927–941.

[51] S. Saitoh, H. Daiguji, E. Hihara, Effect of tube diameter on boiling heat transfer of R-134a in horizontal small-diameter tubes, Int. J. Heat Mass Transfer 48 (2005) 4973–4984.

[52] E. Hihara, C. Dang, Boiling heat transfer of carbon dioxide in horizontal tubes, in: Proc. 2007 ASME–JSME Thermal Eng. Summer Heat Transfer Conf., Canada, HT2007-32885, 2007, pp. 843–849.

[53] A. Greco, Convective boiling of pure and mixed refrigerants: an experimental study of the major parameters affecting heat transfer, Int. J. Heat Mass Transfer 51 (2008) 896–909.

[54] D. Shiferaw, Two-phase flow boiling in small- to micro-diameter tubes, Ph.D. Thesis, Brunel University, UK, 2008.

[55] H. Ohta, K. Inoue, M. Ando, K. Watanabe, Experimental investigation on observed scattering in heat transfer characteristics for flow boiling in a small diameter tube, Heat Transfer Eng. 30 (2009) 19–27.

[56] M. Ducoulombier, S. Colasson, J. Bonjour, P. Haberschill, Carbon dioxide flow boiling in a single microchannel – Part II: heat transfer, Exp. Therm. Fluid Sci. 35 (2011) 597–611.

[57] H.K. Oh, C.H. Son, Flow boiling heat transfer and pressure drop characteristics of CO in horizontal tube of 4.57-mm inner diameter, Appl. Therm. Eng. 31 (2011) 163–172.

[58] J.T. Oh, A.S. Pamitran, K.I. Choi, P. Hrnjak, Experimental investigation on two-phase flow boiling heat transfer of five refrigerants in horizontal small tubes of 0.5, 1.5 and 3.0 mm inner diameters, Int. J. Heat Mass Transfer 54 (2011) 2080–2088.

[59] D. Del Col, S. Bortolin, Investigation of dryout during flow boiling in a single microchannel under non-uniform axial heat flux, Int. J. Therm. Sci. 57 (2012) 25–36.

[60] T.G. Karayiannis, M.M. Mahmoud, D.B.R. Kenning, A study of discrepancies in flow boiling results in small to microdiameter metallic tubes, Exp. Therm. Fluid Sci. 36 (2012) 126–142.

[61] R. Mastrullo, A.W. Mauro, J.R. Thome, D. Toto, G.P. Vanoli, Flow pattern maps for convective boiling of CO_2 and R410A in a horizontal smooth tube: experiments and new correlations analyzing the effect of the reduced pressure, Int. J. Heat Mass Transfer 55 (2012) 1519–1528.

[62] C.B. Tibiriçá, G. Ribatski, J.R. Thome, Flow boiling characteristics for R1234ze(E) in 1.0 and 2.2 mm circular channels, ASME J. Heat Transfer 134 (2012) 020906.

[63] Z. Sun, CO_2 flow boiling heat transfer in horizontal tubes, Ph.D. Thesis, Purdue University, West Lafayette, IN, 2001.

[64] S.H. Yoon, E.S. Cho, Y.W. Hwang, M.S. Kim, K. Min, Y. Kim, Characteristics of evaporative heat transfer and pressure drop of carbon dioxide and correlation development, Int. J. Refrig. 27 (2004) 111–119.

[65] L. Wojtan, T. Ursenbacher, J.R. Thome, Investigation of flow boiling in horizontal tubes: Part I – a new diabatic two-phase flow pattern map, Int. J. Heat Mass Transfer 48 (2005) 2955–2969.

[66] L. Cheng, G. Ribatski, L. Wojtan, J.R. Thome, New flow boiling heat transfer model and flow pattern map for carbon dioxide evaporating inside horizontal tubes, Int. J. Heat Mass Transfer 49 (2006) 4082–4094.

[67] D. Del Col, F. Fantini, L. Rossetto, Dryout quality in a minichannel flow boiling, in: XXV UIT National Heat Transfer Conf., Italy, 2007, pp. 18–20.

[68] L. Cheng, G. Ribatski, J.M. Quibén, J.R. Thome, New prediction methods for CO_2 evaporation inside tubes: part I – a two-phase flow pattern map and a flow pattern based phenomenological model for two-phase flow frictional pressure drops, Int. J. Heat Mass Transfer 51 (2008) 111–124.

[69] S. Jeong, D. Park, Evaporative heat transfer of CO_2 in a smooth and a micro-grooved miniature channel tube, Heat Transfer Eng. 30 (2009) 582–589.

[70] E.W. Lemmon, M.L. Huber, M.O. McLinden, Reference fluid thermodynamic and transport properties – REFPROP Version 8.0, NIST, MD, 2007.

[71] A.S. Kon'kov, Experimental study of the conditions under which heat exchanger deteriorates when a steam-water mixture flows in heated tube, Teploenergetika 13 (1965) 77.

[72] H. Mori, S. Yoshida, K. Ohishi, Y. Kakimoto, Dryout quality and post-dryout heat transfer coefficient in horizontal evaporator tubes, in: European Thermal Science Conf., Germany, 2000, pp. 839–844.